Journal of Natural Fibers

ISSN: (Print) (Online) Journal homepage: https://www.tandfonline.com/loi/wjnf20

Insights on the Hair Keratin Structure Under Different Drying Conditions

José Pedro Carvalho, Carla Silva, Madalena Martins & Artur Cavaco-Paulo

To cite this article: José Pedro Carvalho, Carla Silva, Madalena Martins & Artur Cavaco-Paulo (2023) Insights on the Hair Keratin Structure Under Different Drying Conditions, Journal of Natural Fibers, 20:2, 2250556, DOI: 10.1080/15440478.2023.2250556

To link to this article: https://doi.org/10.1080/15440478.2023.2250556

Published online: 03 Sep 2023.

JOURNAL OF NATURAL FIBERS
2023, VOL. 20, NO. 2, 2250556
https://doi.org/10.1080/15440478.2023.2250556

Insights on the Hair Keratin Structure Under Different Drying Conditions

José Pedro Carvalho[a,b], Carla Silva[a], Madalena Martins[a,b], and Artur Cavaco-Paulo[a,b,c]

[a]Centre of Biological Engineering (CEB), University of Minho, Braga, Portugal; [b]Solfarcos, Pharmaceutical and Cosmetic Solutions, Braga, Portugal; [c]AQUIS Inc., San Francisco, CA, USA

ABSTRACT

It is important to understand the patterns of hair keratin integrity caused by drying methods. No previous information exists in the literature to compare different drying conditions needed to assess physical changes in the hair keratin. We used human hair for these experiments. We found that different drying conditions greatly influence the wearing fatigue of the hair fibers. Using a microfiber towel (80% polyester/20% nylon) to remove the excess water seems to better retain the integrity of human hair when compared to drying with a blow-drier or a cotton towel. Hair dried with a microfiber towel showed strong intensity bands at 1664 cm-1 consistent with an alpha-helix structure, while these bands were absent in the spectrum of the hair dried with a blow-drier or a cotton towel. Fatigue recovery of the hair sample dried with a microfiber towel showed much higher wear resistance when compared with the cotton towel and blow-drier processes. These findings were supported by FTIR (*Fourier transform infrared)* which aided in the elucidation of the secondary structure of alpha-keratin and its effect in the stabilization of hair fibers. When hair samples were exposed to high temperatures, DSC (*Differential Scanning Calorimetry)* profiles provided information about the movement of water molecules from the fiber, being the enthalpy for hair dried with microfiber towel the highest value. Contributions from damage, friction, and heat were correlated with the molecular structure, in particular, the alpha-helixes predicting that drying condition using a microfiber towel is the process that better preserves hair integrity.

KEYWORDS

Keratin fiber; FTIR microscopy; wear resistance; alpha-helix; hair damages; molecular structure

关键词

角蛋白纤维; 显微镜; 耐磨性; α螺旋; 毛发损伤; 分子结构

CONTACT Madalena Martins mms@solfarcos.com Solfarcos, Pharmaceutical and Cosmetic Solutions, Avenida Imac. Conceição 589, Braga 4700-034, Portugal; Artur Cavaco-Paulo artur@ceb.uminho.pt

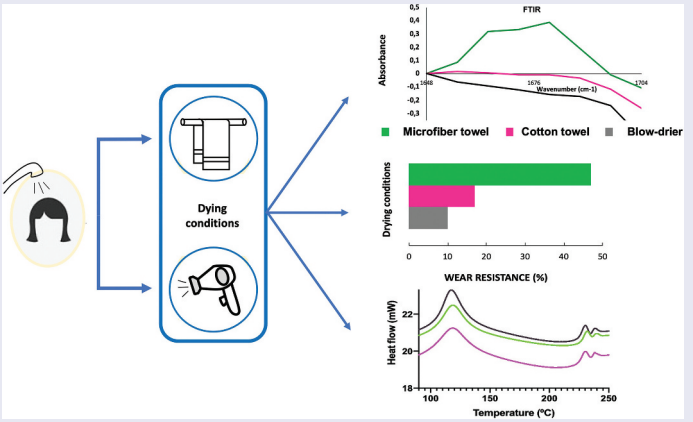

摘要

了解干燥方法引起的头发角蛋白完整性的模式很重要. 文献中没有以前的信息来比较评估头发角蛋白物理变化所需的不同干燥条件。我们用人的头发做这些实验. 我们发现，不同的干燥条件对头发纤维的穿着疲劳有很大影响. 与用吹风机或棉毛巾干燥相比，用超细纤维毛巾（80%聚酯纤维/20%尼龙）去除多余的水分似乎能更好地保持头发的完整性. 用超细纤维毛巾干燥的头发在1664 cm-1处显示出与α-螺旋结构一致的强强度带，而用吹风机或棉毛巾干燥的毛发的光谱中不存在这些带. 与棉毛巾和吹风机工艺相比，用超细纤维毛巾干燥的头发样品的疲劳恢复表现出更高的耐磨性. 这些发现得到了傅立叶变换红外光谱（FTIR）的支持，该光谱有助于阐明α角蛋白的二级结构及其在头发纤维稳定中的作用. 当头发样品暴露在高温下时，DSC（差示扫描量热法）图谱提供了关于水分子从纤维中移动的信息，用微纤维毛巾干燥头发的焓值最高. 损伤、摩擦和热量的贡献与分子结构有关，特别是α螺旋预测，使用超细纤维毛巾的干燥条件是更好地保持头发完整性的过程.

Introduction

Hair strands have an extremely ordered and cylinder-shaped arrangement, composed of inert cells, mostly keratinized, and distributed in an exact and pre-defined architecture. At a molecular level, the rigid arrangement of hair fibers contributes to its mechanical properties' resistance and flexibility. A hair fiber is alive when it is anchored inside the hair follicle on the scalp, otherwise it is considered as dead. When the fiber outsides the scalp and grows, its length is increased at a rate of about 1.0 cm/month (Lima et al. 2019).

Human hair fiber is largely constituted of keratin (65–95%), lipid constituents (about 4% wt.), water (15–35% wt.), and trace elements (less than 1% wt.) (Singh, Wang, and Ng 2017; Velasco et al. 2009). Keratin is comprised of 20 different amino acid side chains, basically containing sulfur as cysteine (Bragulla and Homberger 2009; Cruz et al. 2017b). Keratin proteins are complex natural compounds exhibiting heterogeneous morphological structures. They possess an acidic isoelectric point and generally provide negative charge to the hair surface. The highly organized structure of keratin offers significant resistance to several environments. The amino acid alignment of the keratins present in human hair is distinct from other keratins (for example, human stratum corneum (Jialin et al. 1993)). The greater amount of disulfide bridges of human hair keratins makes the hair structure more tougher and durable, providing valuable thermal, mechanical, and chemical resistance (C. Cruz et al. 2016; Celia F.; Cruz et al. 2017b). The intermediate protein filaments display a distinctly ordered and extended alpha-helical conformation prone to form two-stranded coiled coils, which make the filaments highly flexible

and stress-resistant (Herrmann and Aebi 2016). In agreement with the molecular properties given by these structures, they might substantially determine the mechanical resistance of the hair. The evaluation of the mechanical resistance of the hair fibers is crucial to estimate the performance and effects of hair cosmetic treatments.

Hair is hygroscopic, and considerations such as the stability of the hair fiber configuration, and physical and cosmetic properties of treatments are intrinsically correlated with relative humidity conditions. The hair fiber assembly is rich in hydrophilic groups which enable high absorption of moisture (Gupta 2008; Robbins 2012; Shavandi et al. 2017). Therefore, the water content of the hair fibers is a fundamental factor concerning cosmetic and physical properties (Robbins 2012). Water binding of hair keratin encloses interactions between water molecules and the various protein groups, including the acidic and basic chains and the peptide groups (Bouillon and Wilkinson 2005; Choe et al. 2017). Hair readily swells with water; initially the hair fiber increases along its length in about 2%, while its diameter increases in almost 14% when relative humidity reaches 100% (Bouillon and Wilkinson 2005; Robbins 2012).

The physical-chemical status of the hair fiber is additionally essential to assess the friction effect on hair. The friction coefficient depends on the wet and dry state of the hair shaft and on the cuticle geometry. The relative humidity ratio influences the friction of the hair, being higher within the wet state than within the dry hair state (Velasco et al. 2009).

Here, wear resistance and FTIR (Fourier transform infrared) microscopy are used to analyze the effect on hair strands of three types of the drying processes, namely cotton towel, microfiber towel or blow-drier, after washing with shampoo. Through the observation of changes in the spectral intensity and wavenumber displacement of characteristic bands of the hair fibers, it will be possible to correlate changes in the wear resistance provoked by each drying process. All physical changes were monitored by FTIR microscopy analysis of its components. Finally, a comparison is provided from both tests to correlate the effect of the different drying processes on the integrity of the hair fibers.

Materials and methods

Materials

Asian virgin hair samples were kindly provided by a hairdresser in China. Non-corrodible steel balls (50WW–0015/B/S/A) were supplied from Roaches International (Birstall, West Yorkshire, England). Isopore membrane filters (5.0 µm pore size, hydrophilic polycarbonate membrane, 47 mm diameter) were purchased from Merck Sigma, Spain. All the other reagents were used as received.

Drying procedure

The hair samples were previously overbleached by eight bleaching cycles. The bleaching cycle procedure was commercially available and used as mentioned in the manufacturer instructions (lightening powder was mixed with the oxidizing agent 12% (v/v) hydrogen peroxide and applied over the hair samples). This bleaching procedure was repeated 8 times to obtain an overbleached hair.

Then, the overbleached hair samples (200 mg per hair mesh) were washed with shampoo 0.1%, rinsed with water, and dried under different conditions. After washing, the hair samples were wrapped up in a 100% cotton towel or in a microfiber towel (80% polyester and 20% nylon), both for 7 min. Alternatively, a hair sample was dried using a blow-drier at 60–80°C for 7 min. As control, virgin hair, *i.e.*, original hair without overbleaching treatment, was washed with shampoo 0.1% and dried at room temperature. After each drying process, the fibers were equilibrated at room temperature for 24 h. Each condition was repeated 8 times.

Evaluation of hair resistance to mechanical wear

The effect of the drying processes on the hair resistance to the mechanical wear was expressed in terms of hair mass loss after the mechanical insult (Ribeiro et al. 2021). To that, 10 mg of each hair sample was cut into 0.5 cm fragments and incubated in 700 µL of distilled water in 2 mL Eppendorf tubes with five hardened steel balls. The samples were vortexed under 2500 rpm for 12 h, and the reaction mixture was filtered using a membrane with pore size of 5.0 µm. All the Eppendorf tubes were washed five times with 700 µL of distilled water to prevent material loss. The hair mass loss was determined according to equation 1:

$$\text{Hair mass loss}\,(\%) = \left(\frac{\text{Hi} - \text{Hf}}{\text{Hi}}\right) * 100$$

Where Hi corresponds to the initial dry weight of hair and Hf to the final dry weight of hair present in the polycarbonate membrane filter after drying at 40°C for 12 h. For each condition three replicas were tested.

The wear resistance evaluated as fatigue recovery expressed in percentage was calculated according to equation 2:

$$\text{Fatigue recovery}\,(\%) = 100\% - \text{Hair mass loss}\,(\%)$$

Infrared microscopy

The treated hair samples were embedded into an epoxy resin. Transversal cuts with 15 µm were prepared using a microtome (Microtome Leitz) for each treatment condition. The hair cross-sections (around 10 for each condition) were analyzed using FTIR microscope Spectrum Spotlight 300 IR Imaging System (PerkinElmer), which is suitable to obtain structural and chemical information of proteins' secondary structure (Lee et al. 2018). The FTIR spectra were collected in the continuous scan mode for a spectral range from 4000 to 720 cm^{-1}. The treated results showed FTIR spectra of the Amide I band ranging between 1648 and 1704 cm^{-1}. Each spectrum was collected with an average of 15 repetitive scans with a spectral resolution of 8 cm^{-1}. An IR image was acquired, and a corresponding optical micrograph is shown.

Differential Scanning Calorimetry (DSC)

The thermal properties of hair treated with different drying conditions were investigated using DSC technique. For this analysis, 8 mg of each hair sample (three replicate measurements for each condition) was run on a DSC instrument (DSC 6000, Perkin Elmer) being subjected to a thermal ramp from 25°C to 250°C with a constant heating rate (5°C/min) under an inert nitrogen atmosphere.

Statistical analysis

Statistical analysis was performed using one-way analysis of variance (ANOVA) with postdoc Tukey's test to identify significant differences between the results. Differences were considered statistically significant at a p-value <.05.

Results and discussion

Hair drying conditions can cause hair damage including dryness and friction. In this sense, it is important to analyze the most effective process to dry the hair while minimizing damage. This study assessed changes within the structure of alpha-keratin by FTIR analysis and resistance to mechanical wear of hair after repeated shampooing and drying with a blow-dryer, towel made of 100% cotton, and

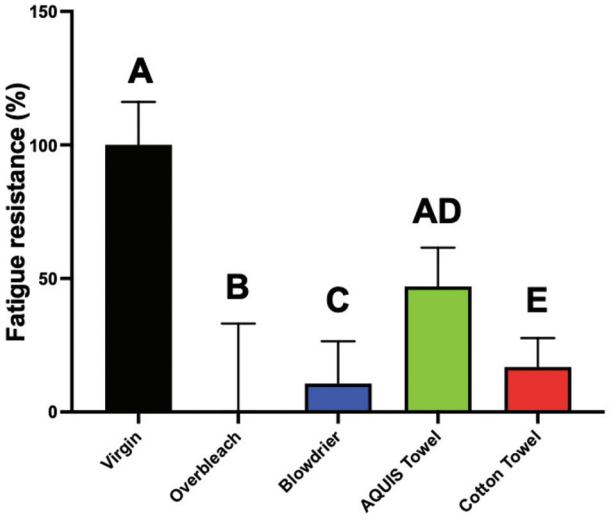

Figure 1. Effect of three drying technologies: cotton towel, microfiber towel, and blow-drier on the resistance of mechanical wear. Grouping information using a Tukey test with 95% confidence, where do not share a letter are significantly different.

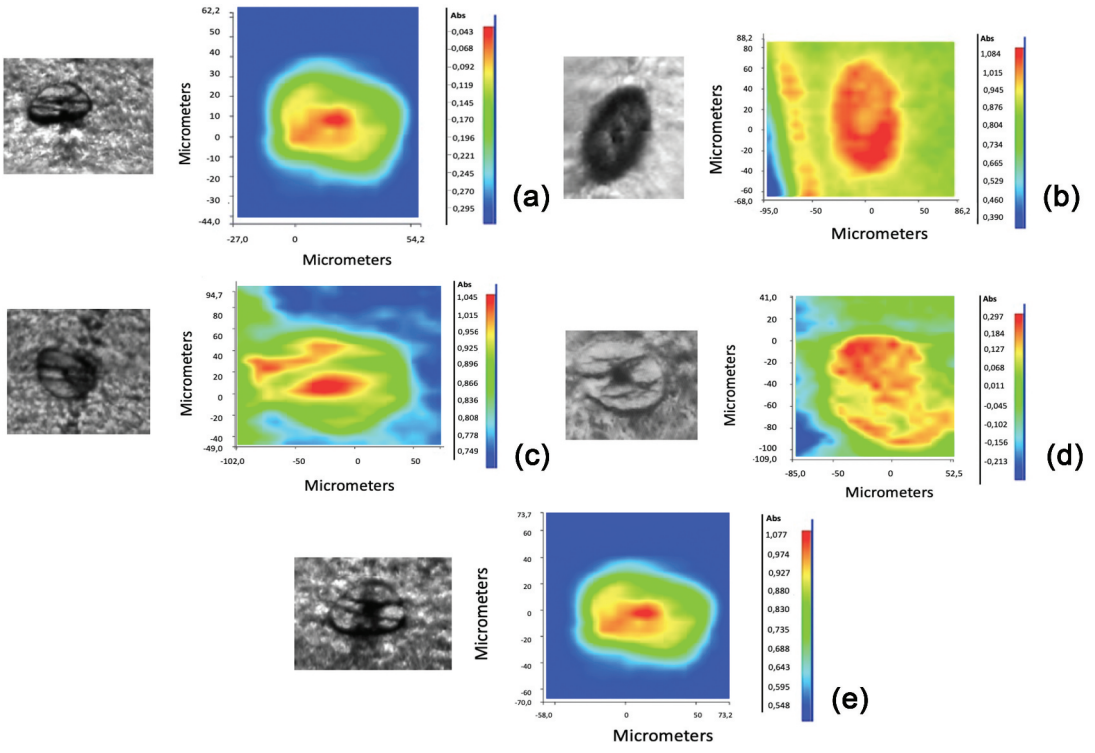

Figure 2. The image on left is the optical image of the cross-section (oval dark area) and on the right chemical imaging from FT-IR microspectroscopy of (a) overbleached hair sample, (b) virgin hair, (c) hair sample dried with a microfiber towel, (d) hair sample dried with blow-drier and (e) hair sample dried with a cotton towel.

microfiber towel made of 80% polyester/20% nylon. The effect of the drying process on the hair resistance to mechanical wear was expressed in terms of hair mass loss after mechanical insult (Figure 1). The hair samples dried with blow-drier exhibited the lowest resistance to mechanical wear (10%) taking into consideration a high protein loss value. Using a cotton towel gave a slightly better result, with 17% resistance to mechanical wear. The hair samples dried with a microfiber towel of 80% polyester/20% nylon presented the higher resistance to mechanical wear (45%) which is statistically significant compared to the other drying conditions.

Asian hair fiber has an outstanding cross-section area among the major ethnic groups of human hair types, exhibiting a circular geometry. The alpha-keratin fiber presents a fibrous organization from a micrometer to a nanometer scale (Franbourg et al. 2003; Leerunyakul and Suchonwanit 2020; C.; Cruz et al. 2016). FTIR microscopy has been applied to cross-sections of hair fibers to investigate the molecular structure of hair strands (Zhang, Senak, and Moore 2011; Barba et al. 2022; Ryu et al. 2016). By spectral mapping associated with the assorted treatments, a FTIR microscope image of the hair was obtained. A visible micrograph of microtomed hair cross-sections is presented in Figure 2 with the corresponding IR and optical image of the hair section.

The analyses of the secondary structure of proteins in the Amide I region from 1600 cm^{-1} to 1700 is a well-stablish method described in major FTIR machinery (Lee et al. 2018; Wilcox, Blanch, and Doig 2016). Amide I represents the vibration caused by the combination of the C=O stretch coupled with a bending of the N-H and C-N planes exhibiting a peak position around 1664 cm^{-1} (Zhang, Senak, and Moore 2011).

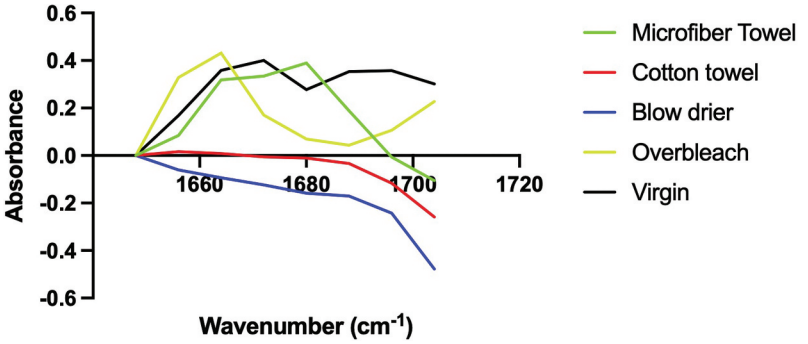

Figure 3. Representative IR spectra obtained from each hair sample treatment microfiber towel of 80% polyester 20% nylon, 100% cotton towel, blow-drier, and the controls overbleach and virgin hair. Each spectrum was obtained from a single pixel and fixed the absorbance as zero for each spectrum.

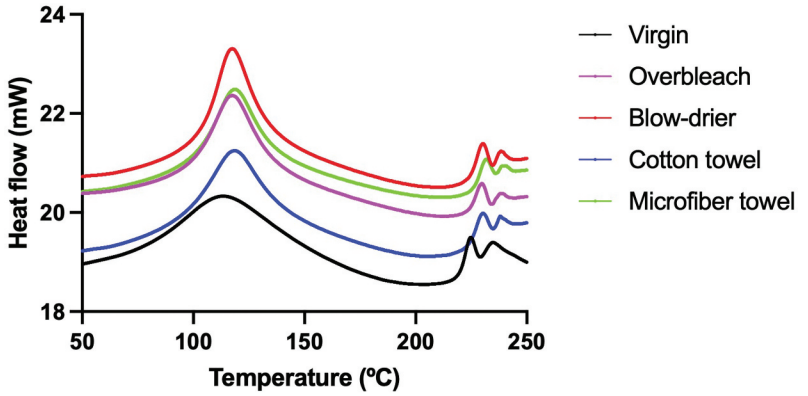

Figure 4. DSC curves recorded for hair treated with Asian hair samples. Each curve is representative from three recorded curves.

Table 1. Melting temperature (°C) and melting enthalpy (J/g) of treated Asian hair, determined from differential scanning calorimetry curves. Each point is the representative value of three values obtained.

Sample	1st Enthalpy (J/g)	1st Temperature (°C)	2nd Enthalpy (J/g)	2nd Temperature (°C)	3rd Enthalpy (J/g)	3rd Temperature (°C)
Virgin	101.4	117.0	6.1	223.7	4.5	233.8
Overbleach	112.3	117.6	7.2	229.7	1.7	238.1
Blow-drier	71.2	117.4	6.3	229.96	1.6	238
Cotton towel	46.3	103	5.7	229.98	3.6	27.2
Microfiber towel	118.4	119.6	5.1	231.26	4.7	236.4

Figure 3 shows the Amide I band ranging between 1648 and 1704 m^{-1}, in which at the wavenumber of 1648 cm^{-1} the intensity was fixed as zero to normalize the band. It was observed that for cotton towel and blow-drier the absorbance value at wavenumbers from 1672 to 1704 cm^{-1} were lower than the absorbance at 1648 cm^{-1} generating a profile with negative absorbances. For the other drying conditions, the peak detection of amide I predicted the alpha-helix content (Figure 3).

It has been presented in FTIR investigations that the absorbance between 1650 and 1659 cm^{-1} is predominantly due to alpha-helical structures, whereas bands in the region 1610–1642 cm^{-1} are largely characteristic of β-structures (Dave et al. 2000; Goormaghtigh, Ruysschaert, and Raussens 2006; Sadat and Joye 2020). Figure 3 exhibits a dominant alpha-helix secondary structure for overbleached and virgin hair (original hair with no treatment) samples, as well as for hair samples treated with microfiber towel condition. The shift absorbance intensity was well defined observing a notable difference between those spectra and the ones from hair treated with blow-drier or cotton towel conditions. For the blow-drier and 100% cotton towel drying processes alpha-helix structures were not detected. Research has suggested that changes in the alpha-helix could be the indication of damage to the hair fiber, which is corroborated by the low wear resistance results depicted above.

Analyzing the spectra obtained by differential scanning calorimetry (DSC) (Figure 4 and Table 1) allows the assessment of relative changes in temperature and energy in the hair samples. Keratin denaturation temperature and enthalpy were recorded by DSC. The denaturation enthalpy depends on the amount and on the structural integrity of the alpha-helical material in the hair structure. It also represents the energy required for the helix denaturation (Cai and Ram Singh 2004; Helan et al. 2014; Lima et al. 2019; Litvinov et al. 2012; Michael and Mantsch 1995). DSC curves of overbleached hair samples dried at room temperature or using a microfiber towel showed similarity in their profile. Nevertheless, slightly higher enthalpy and endothermic peak temperature values were observed for Asian keratin hair samples treated with a microfiber towel. All of the samples showed three endothermic peaks in the temperature range from 50°C to 250°C, corresponding to the different changes in the molecular structure of hair keratin fiber during the heating process (Wortmann et al. 2012). The hair samples dried with a cotton towel presented the lowest values of enthalpy as well as the temperature of the first endothermic peak, as exhibited in Figure 4. The curves display a second and third endotherm peak in the range of 224–238°C which are assigned to the thermal denaturation of alpha-helices and pyrolysis of the matrix, simultaneously (Lima et al. 2018; Singamneni et al. 2019; Tshela Ntumba and Prochoń 2016).

The bleaching process increases the porosity of the hair, which also increases the water absorption causing damage to the hair, including a decrease in protein alpha-helix structure (Dias and FernandaReis 2015; Monteiro, Maciel, and Longo 2005; Tosti et al. 2017).

The first recorded endothermic effect in the temperature of around 120°C indicated the removal of moisture from the hair fiber in which the sample treated with a microfiber towel exhibited a higher enthalpy value (Lima et al. 2018). The blow-drier and cotton towel dried samples exhibited a lower enthalpy and a lower peak temperature, which implies the disorganization of the hair cortical cells (Wortmann, Wortmann, and Popescu 2020). This indicates that higher amount of energy is necessary to start denaturation of hair samples treated with microfiber towel, predicting a slightly lower heat

damage than with the other conditions. These outcomes are in accordance with the previous results showing that samples treated with microfiber towel better preserve the integrity of the hair fiber. The second and third peak temperature (229–238°C) of the overbleach hair are higher than the virgin hair (223–233°C), this can be explained by the fact of the scission of covalent bonds increasing the concentration of cysteic acid, and reflect an increase in the denaturation temperature (Lima et al. 2018; Popescu and Gummer 2016).

The presence of pronounced peak of an alpha-helix structure in FTIR spectra indicates a good integrity of the hair fiber treated with the microfiber towel, and its good wear resistance performance was also demonstrated. For the other dry conditions lower wear resistance and lack of alpha-helix preservation were detected, which in a certain way reflects that the outer layer of the hair fiber was affected by the different drying conditions leading to a reduced protection which was suggested in those results.

Conclusions

In this study, we state that the conditions chosen to dry the hair are crucial to maintain healthy hair fibers after repeated shampooing. The assessment of the mechanical wear resistance using a microfiber towel with the composition of 80% polyester/20% nylon (45% of wear resistance) is statistically different than both other conditions, using a 100% cotton towel or a blow-drier. These last two conditions exhibited the lowest values, 17% and 10%, respectively, predicting hair damages. Similar behaviors were observed from DSC experiments, where cotton towel and blow-drier hair samples decreased the peak temperatures, an indication of hair damages. Hence, these results greatly correlate to FTIR spectra which exhibited the preservation of alpha-helix structure for the microfiber towel dried samples, predicting reduced damages associated with the process. These findings were unexpectable constituting an important domain since no studies exist on the effects of different drying methods on the structure of hair keratin. Future studies are needed to evaluate human hair health outcomes. The use of tools to develop quantitative microbial risk assessment could be suggested to evaluate health exposure potentials and risks relative to these different drying methods.

Acknowledgements

This study was supported by the Portuguese Foundation for Science and Technology (FCT) under the scope of the strategic funding of UIDB/04469/2020 unit and BioTecNorte operation (NORTE-01-0145-FEDER-000004) funded by the European Regional Development Fund under the scope of Norte2020.

Disclosure statement

No potential conflict of interest was reported by the author(s).

Highlights

- different drying conditions deeply affect the wearing fatigue of human hair;
- drying condition with a microfiber towel preserves the alpha-keratin structure of the keratin fiber;
- microfiber towel exhibited higher mechanical wear resistance 45% higher than cotton towel or blow-drier.

References

Barba, C., M. Adria Oliver, M. Martí, M. Kreuzer, and L. Coderch. 2022. Lipid distribution on ethnic hairs by Fourier transform infrared synchrotron spectroscopy. *Skin Research and Technology* 28 (1):75–83. doi:10.1111/srt.13093.

Bouillon, C., and J. Wilkinson. eds. 2005. *The Science of Hair Care*. CRC Press. 10.1201/b14191

Bragulla, H. H., and D. G. Homberger. 2009. Structure and functions of keratin proteins in simple, stratified, keratinized and cornified epithelia. *Journal of Anatomy* 214 (4):516–59. doi:10.1111/j.1469-7580.2009.01066.x.

Cai, S., and B. Ram Singh. 2004. A distinct utility of the amide III infrared band for secondary structure estimation of aqueous protein solutions using partial least squares methods. *Biochemistry* 43 (9):2541–49. doi:10.1021/bi030149y.

Choe, C., J. Schleusener, J. Lademann, and M. E. Darvin. 2017. Keratin-water-NMF Interaction as a three layer model in the human stratum corneum using in vivo confocal raman microscopy. *Scientific Reports* 7 (1):15900. doi:10.1038/s41598-017-16202-x.

Cruz, C., C. Costa, A. Gomes, T. Matamá, and A. Cavaco-Paulo. 2016. Human hair and the impact of cosmetic procedures: A review on cleansing and shape-modulating cosmetics. *Cosmetics* 3 (3):26. doi:10.3390/cosmetics3030026.

Cruz, C. F., M. Martins, J. Egipto, H. Osório, A. Ribeiro, and A. Cavaco-Paulo. 2017b. Changing the shape of hair with keratin peptides. *RSC Advances* 7 (81):51581–92. doi:10.1039/C7RA10461H.

Dave, N., A. Troullier, I. Mus-Veteau, M. Duñach, G. Leblanc, and E. Padrós. 2000. Secondary Structure Components and Properties of the Melibiose Permease from Escherichia Coli: A Fourier transform infrared spectroscopy analysis. *Biophysical Journal* 79 (2):747–55. doi:10.1016/S0006-3495(00)76332-6.

Dias, G., and M. FernandaReis. 2015. Hair cosmetics: An overview. *International Journal of Trichology* 7 (1):2. doi:10.4103/0974-7753.153450.

Franbourg, A., P. Hallegot, F. Baltenneck, C. Toutaina, and F. Leroy. 2003. Current Research on Ethnic Hair. *Journal of the American Academy of Dermatology* 48 (6):S115–S19. doi:10.1067/mjd.2003.277.

Goormaghtigh, E., J.-M. Ruysschaert, and V. Raussens. 2006. Evaluation of the information content in infrared spectra for protein secondary structure determination. *Biophysical Journal* 90 (8):2946–57. doi:10.1529/biophysj.105.072017.

Gupta, B. S. 2008. Textile fiber morphology, structure and properties in relation to friction. In *Friction in textile materials*, 3–36. Elsevier. doi:10.1533/9781845694722.1.3.

Helan, X., S. Cai, X. Lan, and Y. Yang. 2014. Water-stable three-dimensional ultrafine fibrous scaffolds from keratin for cartilage tissue engineering. *Langmuir* 30 (28):8461–70. doi:10.1021/la500768b.

Herrmann, H., and U. Aebi. 2016. Intermediate filaments: Structure and assembly. *Cold Spring Harbor Perspectives in Biology* 8 (11):a018242. doi:10.1101/cshperspect.a018242.

Jialin, Y., Y. Da-Wen, D. M. Checkla, I. M. Freedberg, and A. P. Bertolino. 1993. Human hair keratins. *Journal of Investigative Dermatology* 101 (1):S56–S59. doi:10.1016/0022-202X(93)90501-8.

Leerunyakul, K., and P. Suchonwanit. 2020. Asian hair: A review of structures, properties, and distinctive disorders. *Clinical, Cosmetic and Investigational Dermatology* 13 (April):309–18. doi:10.2147/CCID.S247390.

Lee, Z. H., J. Sheng Kuek, J. Lim, and A. Ming Chua. 2018. "Determination of protein secondary structures using FTIR spectrsoscopy." https://www.shimadzu.com/an/sites/shimadzu.com.an/files/pim/pim_document_file/applications/application_note/13324/apa218043.pdf.

Lima, C. R. R. D. C., R. A. A. de Couto, T. Batello Freire, A. Mari Goshiyama, A. Rolim Baby, M. Valéria Robles Velasco, V. Regina Leopoldo Constantino, and J. Do Do Rosário Matos. 2019. Heat-damaged evaluation of virgin hair. *Journal of Cosmetic Dermatology* 18 (6):1885–92. doi:10.1111/jocd.12892.

Lima, C. R. R. D. C., L. Diva Brocardo Machado, M. Valéria Robles Velasco, and J. Do Do Rosário Matos. 2018. DSC measurements applied to hair studies. *Journal of Thermal Analysis and Calorimetry* 132 (3):1429–37. doi:10.1007/s10973-018-7095-0.

Litvinov, R. I., D. A. Faizullin, Y. F. Zuev, and J. W. Weisel. 2012. The α-Helix to β-Sheet transition in stretched and compressed hydrated fibrin clots. *Biophysical Journal* 103 (5):1020–27. doi:10.1016/j.bpj.2012.07.046.

Michael, J., and H. H. Mantsch. 1995. The use and misuse of FTIR spectroscopy in the determination of protein structure. *Critical Reviews in Biochemistry and Molecular Biology* 30 (2):95–120. doi:10.3109/10409239509085140.

Monteiro, V. F., A. P. Maciel, and E. Longo. 2005. thermal analysis of caucasian human hair. *Journal of Thermal Analysis and Calorimetry* 79 (2):289–93. doi:10.1007/s10973-005-0051-9.

Popescu, C., and C. Gummer. 2016. DSC of human hair: A tool for claim support or incorrect data analysis? *International Journal of Cosmetic Science* 38 (5):433–39. doi:10.1111/ics.12306.

Ribeiro, A., M. Martins, A. Tinoco, and A. Cavaco-Paulo. 2021. Hair resistance to mechanical wear. *Wear* 470–471 (April):203612. doi:10.1016/j.wear.2021.203612.

Robbins, C. R. 2012. *Chemical and physical behavior of human hair*. Berlin, HeidelbergBerlin Heidelberg: Springer. doi:10.1007/978-3-642-25611-0.

Ryu, S. R., W. Jang, S.-I. Yu, B.-H. Lee, O.-S. Kwon, and K. Shin. 2016. FT-IR microspectroscopic imaging of cross-sectioned human hair during a bleaching process. *Journal of Cosmetics, Dermatological Sciences and Applications* 6 (05):181–90. doi:10.4236/jcdsa.2016.65023.

Sadat, A., and I. J. Joye. 2020. Peak fitting applied to Fourier transform infrared and raman spectroscopic analysis of proteins. *Applied Sciences* 10 (17):5918. doi:10.3390/app10175918.

Shavandi, A., T. H. Silva, A. A. Bekhit, and A. E.-D. A. Bekhit. 2017. Keratin: Dissolution, extraction and biomedical application. *Biomaterials Science* 5 (9):1699–735. doi:10.1039/C7BM00411G.

Singamneni, S., R. Velu, M. Prasad Behera, S. Scott, P. Brorens, D. Harland, and J. Gerrard. 2019. Selective laser sintering responses of keratin-based bio-polymer composites. *Materials & Design* 183 (December):108087. doi:10.1016/j.matdes.2019.108087.

Singh, V., S. Wang, and K. W. Ng. 2017. 2.25 Keratin as a biomaterial. In *Comprehensive biomaterials II*, 542–57. Elsevier. doi:10.1016/B978-0-12-803581-8.09317-6.

Tosti, A., A. Juliano, L. David Bloch, and M. Canales. 2017. Cosmetic approach for healthy and damaged hair. *In* 433–48. doi:10.1007/978-3-319-12589-3_26.

Tshela Ntumba, Y.-H., and M. Prochoń. 2016. The effect of modified keratin on the thermal properties of a cellulosic–elastomeric material. *Journal of Thermal Analysis and Calorimetry* 125 (3):1151–60. doi:10.1007/s10973-016-5590-8.

Velasco, M. V. R., T. C. D. S. Dias, A. Zanardi de Freitas, N. D. Vieira Júnior, C. A. S. de Oliveira Pinto, T. Mary Kaneko, and A. Rolim Baby. 2009. Hair fiber characteristics and methods to evaluate hair physical and mechanical properties. *Brazilian Journal of Pharmaceutical Sciences* 45 (1):153–62. doi:10.1590/S1984-82502009000100019.

Wilcox, K. E., E. W. Blanch, and A. J. Doig. 2016. Determination of protein secondary structure from infrared spectra using partial least-squares regression. *Biochemistry* 55 (27):3794–802. doi:10.1021/acs.biochem.6b00403.

Wortmann, F. J., G. Wortmann, J. Marsh, and K. Meinert. 2012. Thermal denaturation and structural changes of α-helical proteins in keratins. *Journal of Structural Biology* 177 (2):553–60. doi:10.1016/j.jsb.2011.09.014.

Wortmann, F. J., G. Wortmann, and C. Popescu. 2020. Linear and Nonlinear Relations between DSC parameters and elastic moduli for chemically and thermally treated human hair. *Journal of Thermal Analysis and Calorimetry* 140 (5):2171–78. doi:10.1007/s10973-019-08252-2.